Check for updates

Two-dimensional Cu nanostructures for efficient photo-catalytic degradation of methylene blue

Mohammed Rehaan Chandan, [ID] Kodi Rajesh Kumar and Aabid Hussain Shaik [ID] *

This work reports the synthesis of stable oxidation-resistant two-dimensional copper (Cu) nanostructures using non-toxic reducing agents and a rapid and simple chemical reduction technique by replacing conventional solvothermal methods. The formation of two-dimensional Cu nanostructures such as Cu nanosheets was successfully observed by tuning the sodium hydroxide (NaOH) and surfactant (CTAB) concentrations during the synthesis process. It has been observed that a high concentration of NaOH (~2 M) is essential to produce stable Cu nanosheets through the oriented attachment mechanism. The morphology of Cu nanosheets was characterized using a transmission electron microscope. Cu nanosheet phase purity and thickness were analysed using XRD and AFM techniques. Moreover, these Cu nanosheets exhibited efficient photocatalytic activity in degrading the methylene blue (MB) dye from synthetic wastewater. The large surface area associated with Cu nanosheets and their two-dimensional structure helps to enhance the photocatalytic activity and MB dye degradation upon solar and UV light irradiation as compared to zero and one-dimensional Cu nanostructures. Almost 95% degradation efficiency has been successfully observed by irradiating the MB dye solution under solar light for 20 min. Cu nanosheet powder was also successfully recycled for degrading the MB dye by centrifuging the degraded solution, and the recycled Cu nanosheets exhibit ~80% degradation under solar light irradiation.

Environmental significance

The work deals with the synthesis of 2D Cu nanostructures using a chemical reduction method for its application in dye degradation. Dyes in effluent pose a serious threat to water bodies and their aquatic ecosystems. Dyes are also carcinogenic in nature if they come in contact with the palatable water. Therefore, the developed material can efficiently degrade the dye under sunlight *via* the photocatalytic effect. Additionally, the nanostructures prepared using the chemical reduction method can be scaled to a larger quantity because of their lower cost.

1. Introduction

Two-dimensional nanostructures such as nanosheets find many applications in various fields due to their unique physical, chemical, optical, and electrical properties associated with the nanoscale dimensions in their diameter and thickness compared to zero and one-dimensional nanostructures such as spherical nanoparticles, nanorods, and nanowires. These applications include fabrication of nanodevices,[1,2] formation of transparent conducting electrodes,[3,4] lithium ion batteries,[5,6] energy storage devices,[7,8] desulphurization of fuel[9] *etc.* In the past few decades, extensive work has been conducted using prominent two-dimensional nanostructures such as graphene/graphene oxide for various applications.[10] Even though a sufficient amount of research has been conducted on graphene-based 2-D nanostructures, interest has been created recently in searching for new materials to replace them due to their

complex synthesis procedure and high costs. To overcome this issue, copper has been considered a suitable material for graphene-based nanosheets due to its low cost and simple synthesis techniques. Also, the research conducted on the synthesis of copper nanosheets as an alternate efficient 2-D structure for graphene is very sparse due to copper's unique easy oxidation behaviour. This work focuses on synthesizing stable oxidation resistant Cu nanosheets as a substitute for graphene-based nanosheets.

Despite applications, the synthesis of 2-D nanostructures such as nanosheets is a complex issue. Various methods are available to prepare nanosheets. These include the solvothermal method,[11] chemical bath deposition,[12] thermal decomposition,[13] sonochemical method,[14] exfoliation method[15] *etc.* Tang *et al.* have synthesized graphene oxide nanosheets using the hydrothermal method.[16] Dubal *et al.* have reported that multilayer metal oxide nanosheets, such as copper oxide nanosheets, could be prepared using the chemical bath deposition method.[17] Wang *et al.* have proposed that graphene-based nanosheets can be prepared by thermally decomposing citric

Colloids and Polymers Research Group, School of Chemical Engineering, Vellore Institute of Technology, Vellore, TN, India. E-mail: aabidhussain.s@vit.ac.in

acid at various high temperatures.[18] Krishnamoorthy et al. have reported that graphene nanosheets could be synthesized from graphene oxide nanosheets by reducing graphene oxide by ultrasonication.[19] Layered MoS_2 nanosheets were also synthesized by applying the shearing exfoliation technique by Li et al.[20] The methods discussed above for the synthesis of nanosheets mainly focus on graphene-based and oxide-based nanosheets. These synthesis procedures involve highly complex techniques such as heating at high temperatures for a prolonged duration and applying shearing for exfoliation. Hence, in this work, we focus on replacing graphene-based and oxide-based nanosheets with cost-effective metal-based nanosheets such as Cu nanosheets by employing simple and rapid techniques for their synthesis.

A few reports were available in the literature to synthesize copper nanosheets using simple and rapid techniques. Shaik and Chakraborty (2016) suggested a simple and rapid room temperature reduction technique for synthesizing Cu nanosheets by reducing $Cu(OH)_4^{2-}$ with hydrazine hydrate in the presence of CTAB at room temperature.[21] Recently, Lee et al. (2021) synthesized Cu nanosheets using food-grade chemicals such as methylsulfonylmethane ($DMSO_2$) and NaOH and LiOH as reducing agents.[22] This method requires 2 hours of reaction time for producing Cu nanosheets. Although these two methods are simple, these procedures involve using toxic chemicals such as hydrazine hydrate[21] and a reaction time of more than 2 hours.[22] This work proposes a simple and rapid reduction technique for synthesizing Cu nanosheets in 1 hour by replacing toxic reducing agents such as hydrazine hydrate and sodium borohydride with non-toxic reducing agents such as ascorbic acid.

Moreover, these 2-D nanostructures, such as nanosheets, mainly focus on fabricating energy storage devices. However, the application of nanosheets in wastewater treatment, i.e., removing textile dyes from wastewater, is very limited. The removal efficiency of dye can be improved by increasing the surface area through surface modification. Manippady et al. (2020) prepared hybrid mesoporous magnetic nanosheets by carbonization of bagasse and claimed that these nanosheets are efficient in removing the Congo red and methylene blue dyes from wastewater (more than 90%) within 24 min.[23] Lei et al. (2013) reported that oils, organic solvents, and dyes could be removed from wastewater using porous boron nitride nanosheets.[24] Wang et al. (2019) state that the wastewater can be purified in terms of dye using hierarchical micro- and mesoporous carbon nanostructures such as N-doped carbon nanosheets with a high specific surface area.[25] Dang et al. (2019) prepared WS_2 nanosheets using the hydrothermal method and claimed that these nanosheets are highly efficient in removing methylene blue dye from waste water.[26] In addition, several researchers have also conducted various studies on different nanomaterials towards dye degradation.[27–39]

From the foregoing discussion, it has been observed that most of the studies were reported on removing the textile dye from wastewater using hybrid nanosheets synthesized using toxic chemicals and complex heat treatment methods that are not cost-effective. No work has been reported to remove textile dyes such as methylene blue dye using cost-effective metal nanosheets such as copper nanosheets. In addition, rapid MB dye degradation could be possible due to the combined adsorption due to larger surface area and degradation effect due to light intensity. In this work, we propose a simple, rapid, and toxic chemical-free usage technique for synthesizing copper nanosheets to efficiently remove the methylene blue dye. Cu nanosheets produced in this work show better removal efficiency in MB dye removal, which is on par with the hybrid nanosheets produced using very expensive and prolonged synthesis techniques.

2. Experiments

2.1. Materials required

Copper chloride dihydrate ($CuCl_2 \cdot 2H_2O$), ascorbic acid, and cetyltrimethylammonium bromide were purchased from Sigma-Aldrich, India. Sodium hydroxide was procured from SD Fine Chemicals, India. Ethanol of AR grade 99.9% purity was obtained from Jiangsu Huaxi International, China. Methylene blue dye was received from Merck Chemicals, India. The chemicals received were used as received without performing any purification procedures.

2.2. Deoxygenation of solvents

The solvents used to synthesize Cu nanosheets were purged with inert gases (N_2/Ar) for 30 min before synthesis to reduce the dissolved oxygen concentration present in the solvents. After purging with inert gases, dissolved oxygen in the solvents was reduced to less than 1 mg l^{-1}, as confirmed by the measurements of dissolved oxygen.

2.3. Synthesis of Cu nanosheet powder

Cu nanosheet powder was synthesized by modifying the already published protocol by Shaik and Chakraborty (2016).[21] Initially, a sodium hydroxide (NaOH) solution of 2 M was prepared in 100 ml of water. Then 1.5 mmol of copper chloride dihydrate ($CuCl_2 \cdot 2H_2O$) was weighed, added to the above NaOH solution, and stirred continuously for 10 min until the copper salt completely dissolved. After the dissolution of copper salt in NaOH solution, 5 mmol of cetyltrimethylammonium bromide (CTAB) surfactant was weighed and mixed with the above solution under vigorous stirring for 20 min until the complete dissolution of CTAB. Later, the above solution was reduced by adding 10 ml of 3 M ascorbic acid reducing agent solution. After the addition of the reducing agent solution, the color of the solution starts to turn into a brick red color from the blue color Cu $(OH)_4^{2-}$ solution indicating the formation of Cu nanosheets in the aqueous solution. Later, the above solution was transferred to centrifuge tubes and centrifuged at 10 000 rpm for 10 min. After 10 min, the supernatant solution was discarded from the tubes, and the paste attached to the powder was redispersed in ethanol solution and centrifuged again for 10 min at 10 000 rpm. Finally, the Cu nanosheet paste attached to the centrifuge tubes was collected and dried in an inert gas environment to recover Cu nanosheet powder.

2.4. Photocatalytic degradation of methylene blue dye using Cu nanosheet powder

Degradation of methylene blue dye was performed by exposing the dye solution containing Cu nanosheet powder under solar and UV light. Initially, the synthetic wastewater was prepared by adding MB dye to water (40 ppm concentration). Later, the above solution was mixed with the required amount of Cu nanosheets powder (different mass concentrations ranging from 0.1–1 wt%). The above solution was stirred continuously under magnetic stirring for 1 hour to reach equilibrium. Next, the above solution was irradiated using UV light and solar light for 2 hours by exposing the solution to these lights. At regular intervals of time, the sample was collected and its concentration was measured using a UV-vis spectrophotometer. Based on the initial and final concentrations, the degradation efficiency of methylene blue dye was measured.

2.5. Characterization

The optical properties, photoluminescence, energy band gap and dye concentration were measured using a UV-vis spectrophotometer (Shimadzu 1800). The morphology of Cu nanosheets was characterized using a transmission electron microscope (Tecnai G2 20S Twin). The thickness of Cu nanosheets was measured using an atomic force microscope (Agilent Technologies, Model-5500, USA). The phase purity of Cu nanosheet powder was analyzed using the X-ray diffraction technique (Philips PW-17291710). The concentration of dissolved oxygen present in water was measured using a probe type dissolved oxygen meter (HACH).

3. Results and discussion

3.1. Synthesis of Cu nanosheets

Two-dimensional Cu nanostructures were synthesized by employing a simple reduction technique using a non toxic
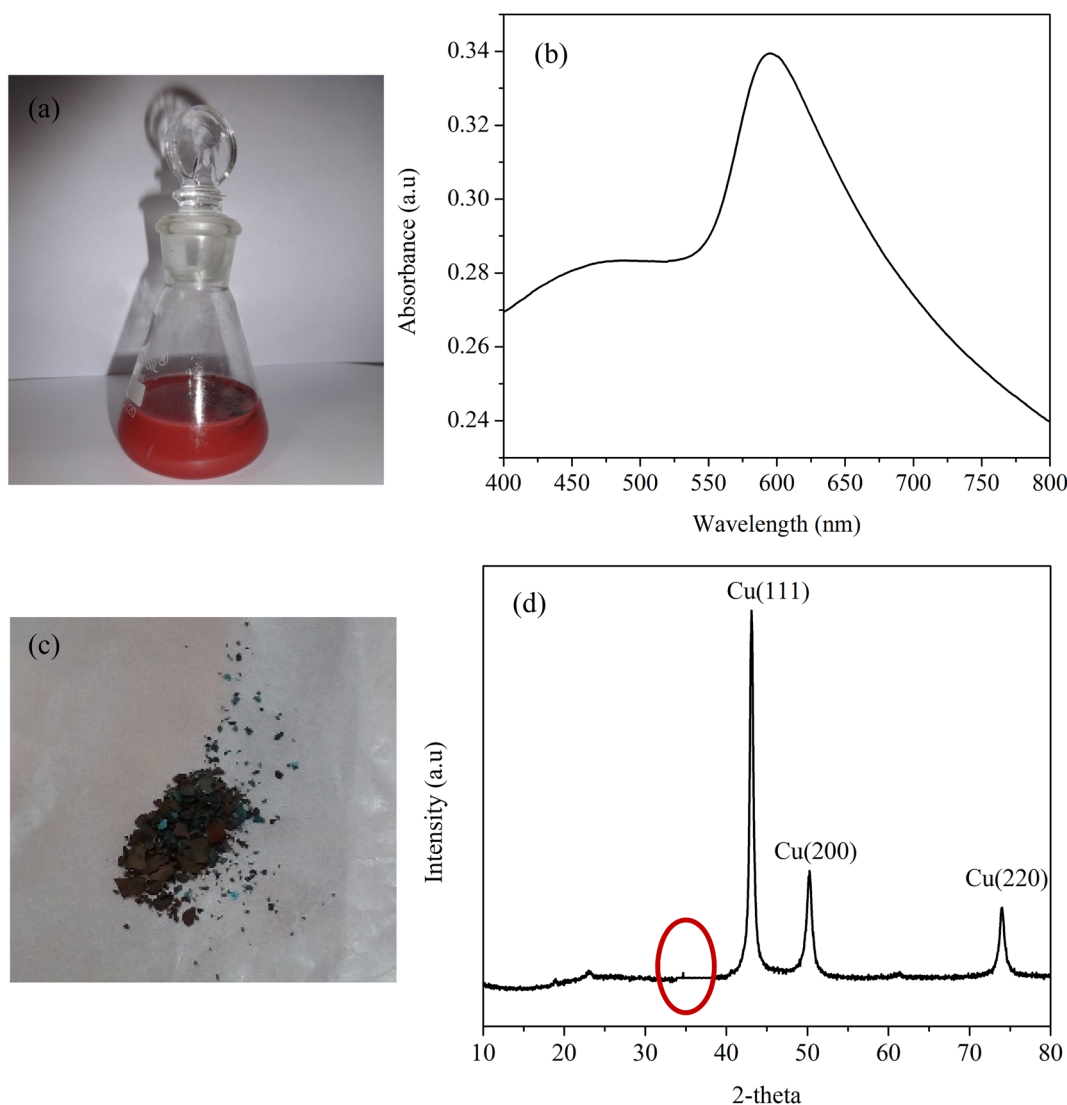

Fig. 1 (a) Digital image of Cu nanosheets in an aqueous phase, (b) UV-vis spectra, (c) digital image of Cu nanosheet powder and (d) XRD spectra of Cu nanosheets.

reducing agent. This method helps in replacing conventional methods such as the hydrothermal method for preparing two-dimensional nanostructures that require high heating temperatures and prolonged reaction times. Despite synthesis, Cu nanosheets find some limitations due to their quick oxidizing nature. Hence it is very challenging to protect the Cu nanosheets from being oxidized. In this work, Cu nanosheets were shielded from oxidation by purging the solvents with inert gases and performing the entire synthesis in an inert gas environment. In addition to purging, oxidations of Cu nanosheets were also minimized by protecting the surface of Cu nanosheets with sterically stabilized surfactants such as CTAB. The selective adsorption of CTAB on the surface helps in two-dimensional growth of nanosheets. Additionally, it also helps in minimising the surface oxidation of Cu nanosheets by providing a protective layer on the surface.

Fig. 1(a) represents the digital image of the synthesized Cu nanosheets in the aqueous phase. The initial indication of the presence of Cu nanosheets in water was confirmed by measuring the surface plasmon resonance peak using a UV-vis spectrophotometer, as shown in Fig. 1(b). From the figure, a surface plasmon resonance peak at 595 nm was observed suggesting the formation of Cu nanosheets in water. Next, Cu nanosheet powder was prepared by centrifuging the Cu nanosheet sol and drying using inert gas purging, as shown in Fig. 1(c). The phase purity of Cu nanosheet powder obtained after centrifugation of Cu nanosheet sol was measured using X-ray diffraction, as shown in Fig. 1(d). The XRD plot from Fig. 1(d) shows the diffraction peaks at 43°, 50.4°, and 74.2°, which corresponds to (1 1 1), (2 0 0), and (2 2 0) faces of pure copper (JCPDS: 04-0836). Since Cu is an easily oxidizable metal, there is a possibility of surface oxidation. This was also observed in our XRD studies where it shows a small peak at a diffraction angle of 36° (highlighted in Fig. 1(d)) suggesting the formation of a Cu_2O layer on the surface of the Cu nanostructure along with pure Cu peaks. Also, as observed from our previous work

(XPS study on copper), a minimal surface oxidation occurs leaving bulk pure copper.[40] This confirms that the Cu nanosheets are highly stable against aggregation and oxidation with minimum surface oxidation.

The morphology of the as-synthesized Cu nanosheets was measured using a transmission electron microscope, as shown in Fig. 2(a). The TEM image from Fig. 2(a) clearly demonstrates that the formed structures are elongated, such as nanosheets with a length of 650 nm and diameter of 150 nm. And also, the thickness of the nanosheets is very thin, as observed from the TEM image. HRTEM analysis of Cu nanosheets was also conducted to confirm that the nanosheets are mostly formed due to the growth in 2-dimensions, which has been observed from the uniform fringe structure at a larger distance, as shown in Fig. 2(b). The HRTEM image shows the uniform fringe structure pattern over a larger distance with a d-spacing of 0.21 nm which correspond to the 111 plane of Cu as obtained from XRD spectra, suggesting Cu nanosheet growth.

The exact thickness of Cu nanosheets was characterized using an atomic force microscope, as shown in Fig. 3. As shown in the figure, the Cu nanosheets exhibit a thickness of 13 nm, which is well consistent with the data obtained from TEM analysis.

The concentration of NaOH greatly influences the growth of Cu nanosheets. In order to probe this effect, Cu nanosheets were prepared by varying the NaOH concentration from 0.5–3 M NaOH. Fig. 4 represents the TEM images of Cu nanostructures synthesized at various concentrations of NaOH. The figure shows that the spherical nanoparticles and one-dimensional nanostructures such as nanorods were observed at 0.5 M and 1 M concentrations of NaOH, as shown in Fig. 4(a) and (b). If the NaOH concentration reaches 2 M, two-dimensional structures such as thin and large nanosheets were observed as shown in Fig. 4(c). However, the diameter and length of the nanosheets were drastically reduced for the Cu nanostructures synthesized with a 3 M NaOH concentration, as shown in Fig. 4(d). This
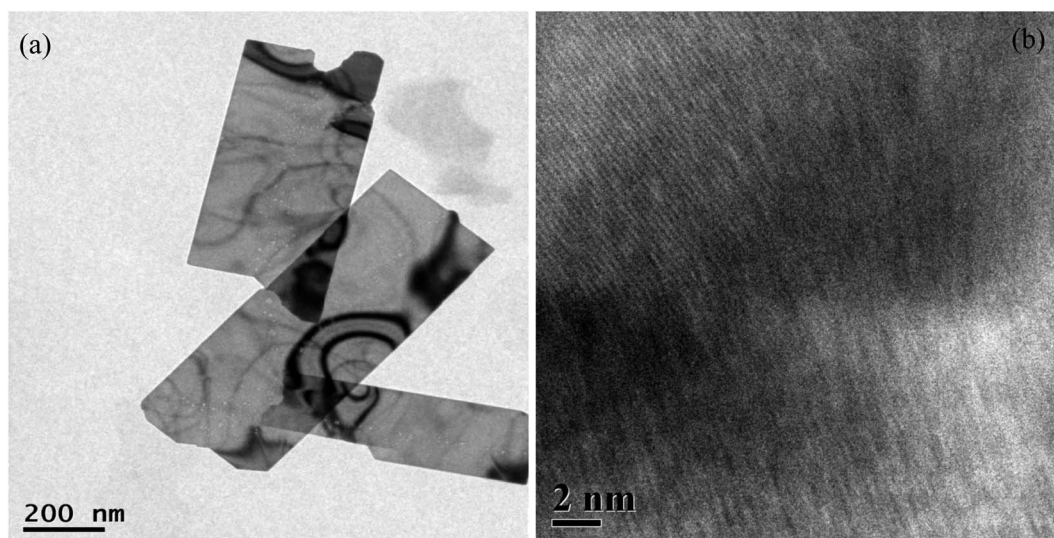

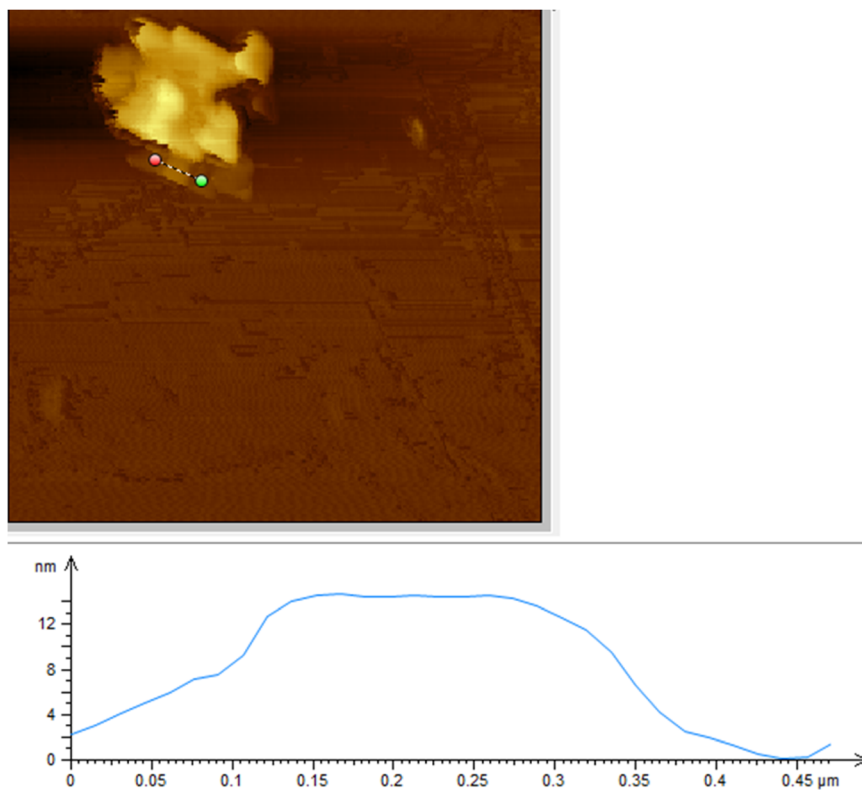Fig. 2 (a) TEM and (b) HRTEM images of Cu nanosheets.

Fig. 3 Atomic force microscopy image of Cu nanosheets.

confirms that the variation of pH due to different NaOH concentrations promotes Cu nanostructure growth due to the oriented attachment mechanism of spherical particles with respect to the NaOH concentration. A similar mechanism has also been reported in the literature with respect to the NaOH concentration on crystal growth.[41]

3.1.1. Checking the suitability of Cu nanosheets as a photocatalyst using band gap energy. The band gap energy of the synthesized 2D Cu nanostructures was calculated using the Tauc equation from UV-vis spectroscopy data. The Tauc plot ($h\nu$ vs. $(\alpha h\nu)^2$) was generated from the UV-vis data as shown in Fig. 5. From the plot, a band gap energy of 2.78 eV is noticed for the as synthesized Cu nanosheets. Even though it is less than those of semiconductor nanomaterials such as ZnO and TiO$_2$ nanostructures, it can be considered as an excellent photocatalyst for dye removal from waste water due to its larger aspect ratio and surface area.

3.2. Degradation of methylene blue dye using Cu nanosheet powder

In this work, degradation of methylene blue dye was performed through the photocatalytic process by irradiating the dye solution using Cu nanosheet powder under UV light and sunlight. Prior to degradation studies, 40 ppm of methylene blue dye solution was prepared by dispersing a known amount of methylene blue dye powder in water. After preparing the required concentration of dye solution, the synthesized

photocatalyst such as Cu nanosheet powder of different mass concentrations was added to the above dye solution and constantly stirred for 1 hour under dark conditions using a magnetic stirrer to achieve equilibrium. After that, the degradation of the dye solution was performed by irradiating the conical flask containing Cu nanosheet powder using UV and solar light. The degradation efficiency was calculated in terms of percentage using the following formula.

$$\text{Degradation efficiency}(\%) = \frac{C_0 - C}{C_0} \times 100$$

where, C_0 = initial concentration of dye solution and C = final concentration of dye solution.

Initially, degradation of methylene blue with aqueous synthetic water was performed by adding Cu nanosheet powder to the dye solution followed by not irradiating the dye solution under UV and solar light, as shown in Fig. 6. After adding Cu nanosheet powder, the sample was collected at regular intervals of time from the flask and measured for its concentration using a UV-vis spectrophotometer. Fig. 6 shows the concentration and degradation profiles of methylene blue dye solution without irradiation. From the figure, it can be seen that the degradation efficiency is ∼40%, which is very low, and also, the time required for degradation is very high, which consumes ∼90 min, as shown in Fig. 6. This could possibly be due to the adsorption of dye molecules on the surface of Cu nanosheets associated with a larger surface area as compared to zero dimensional (spherical nanoparticles) and one dimensional
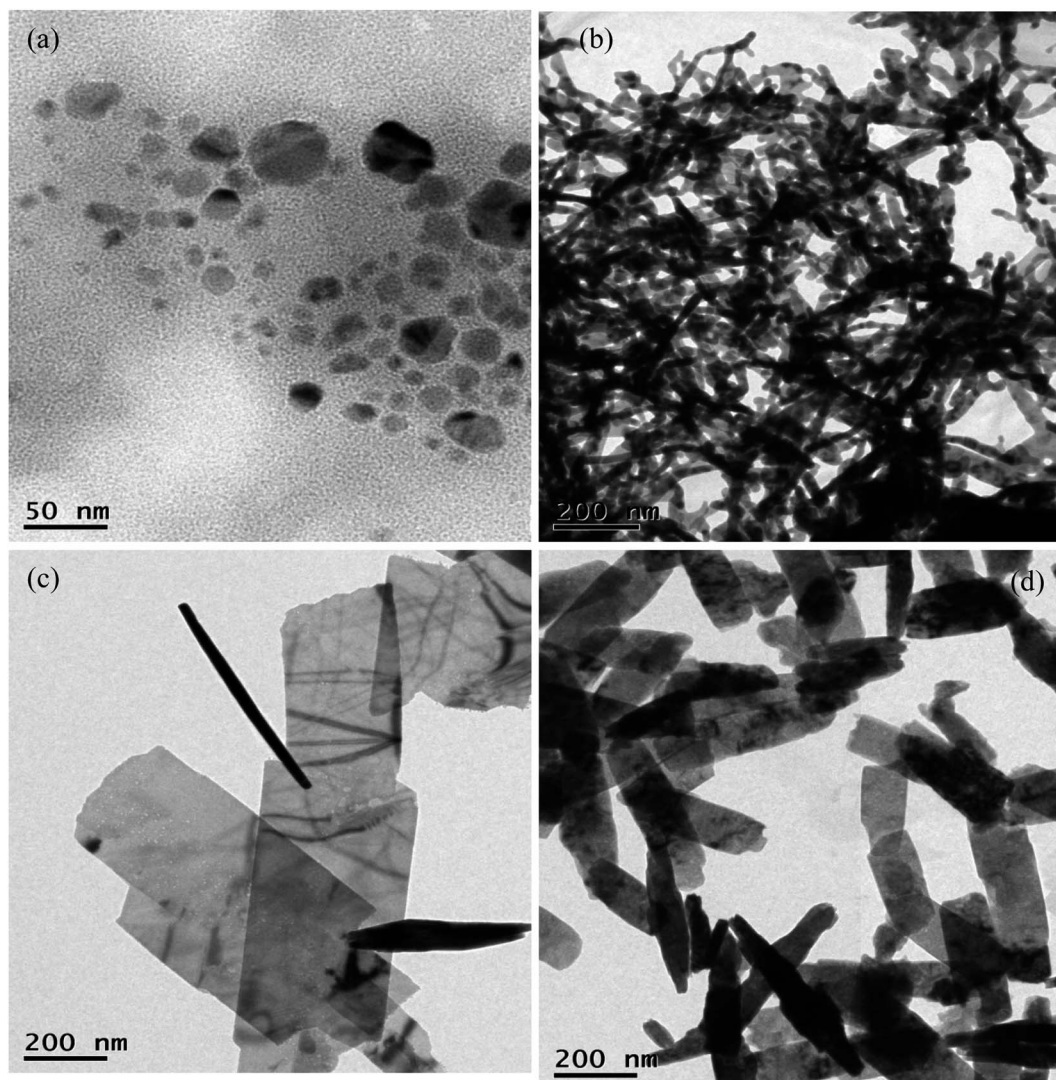
818 | *Environ. Sci.: Adv.*, 2022, **1**, 814–826

© 2022 The Author(s). Published by the Royal Society of Chemistry

Fig. 4 TEM image of Cu nanosheets synthesized at (a) 0.5 M (b) 1 M (c) 2 M and (d) 3 M NaOH concentrations.
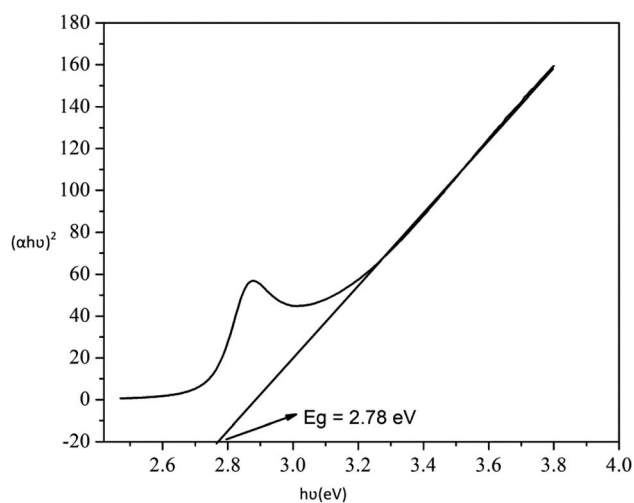

Fig. 5 Tauc plot for the energy band gap of synthesized Cu nanosheets.

structures (nanorods) which helps in more adsorption of dye molecules on the surface of Cu nanosheets. Also, degradation experiments were conducted in an open beaker without sealing the mouth of the beaker allowing the light to enter the beaker.

Next, the degradation of MB dye solution containing different mass concentrations of Cu nanosheet powder was performed by irradiating the synthetic dye solution under UV light and solar light, as shown in Fig. 7. Fig. 7 represents the photocatalytic degradation of methylene blue dye solution using Cu nanosheet powder under UV light (9 W mercury lamp as a light source) concerning different mass concentrations of Cu nanosheet powder in the synthetic dye solution. From the figure, it can be seen that the degradation efficiency increases with an increase in the concentration of Cu nanosheet powder. Moreover, a maximum degradation of ~75% was observed within 45 minutes compared to degradation that occurred without irradiation. The main reason for this high efficiency and low degradation time could possibly be due to the combined adsorption and degradation effect. Since we have
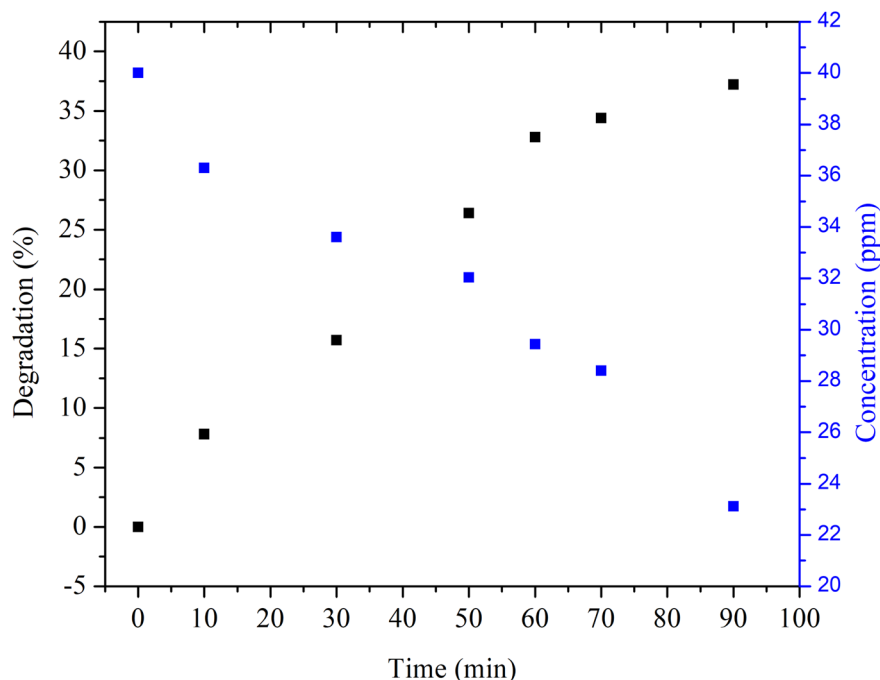
Fig. 6 Degradation and concentration profiles of MB dye using Cu nanosheet powder without irradiation.

used 2-dimensional Cu nanostructures such as Cu nanosheets for removing the dye from the aqueous solution, these 2-dimensional structures have a large surface area as compared to zero dimensional (spherical nanoparticles) and one dimensional structures (nanorods) thereby helping in more adsorption of dye molecules on the surface of Cu nanosheets. In

addition, degradation due to UV irradiation also accelerates the MB dye removal efficiency. Due to this combined effect, dye removal efficiency was enhanced under UV light irradiation as compared to that without irradiation.

However, a sudden and rapid reduction in the degradation time of ~20 min and an increase in the degradation efficiency of
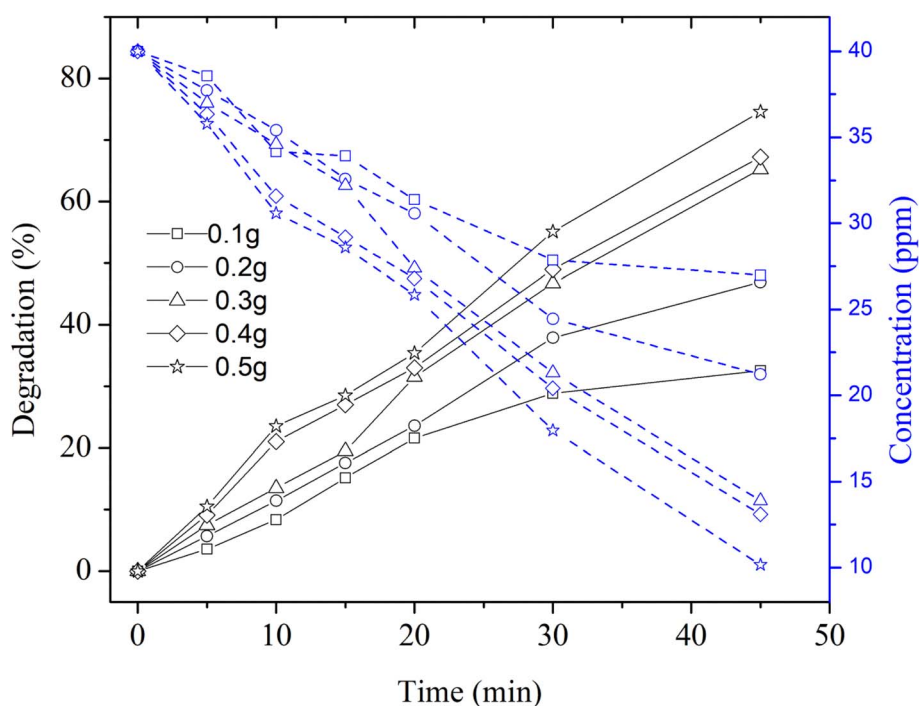

Fig. 7 Degradation and concentration profiles of MB dye using Cu nanosheet powder of different weights under UV irradiation.
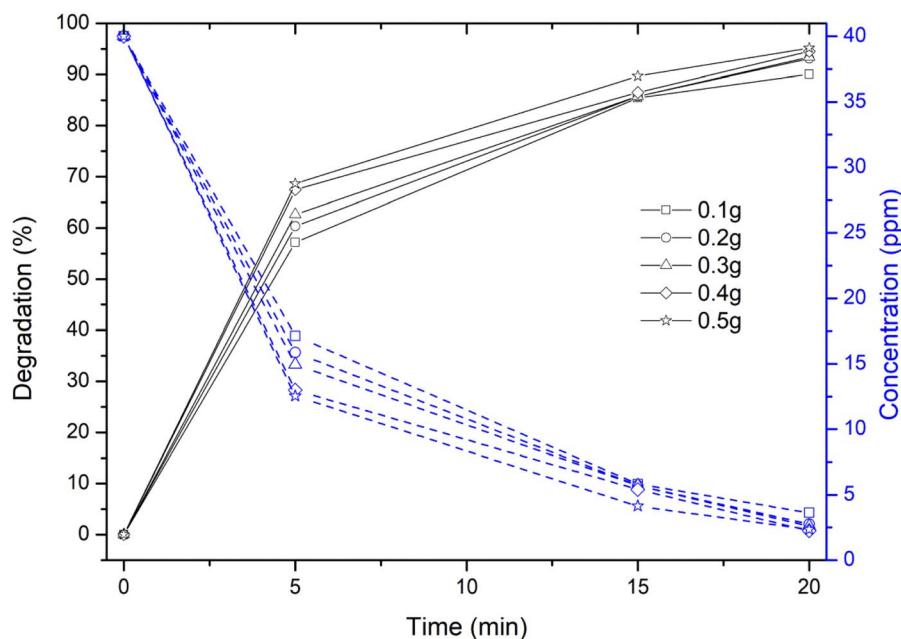
Fig. 8 Degradation and concentration profiles of MB dye using Cu nanosheet powder of different weights under solar irradiation.

~95% has been observed due to the irradiation of dye solution containing Cu nanosheet powder under solar light irradiation as shown in Fig. 8. This could possibly be due to the high intensity of solar light and the adsorptive catalytic behaviour of Cu nanosheets due to their 2-dimensional structure.

3.3. Degradation of methylene blue dye using recycled Cu nanosheet powder

Next, we tried to investigate the effect of recycled Cu nanosheets on dye degradation efficiency. To examine this effect, recycled Cu nanosheet powder was prepared from the already irradiated dye solution through centrifugation at 10 000 rpm for 30 min, followed by drying by inert gas purging. After drying, the recycled Cu nanosheet powder was further used to irradiate the dye solution under UV and solar light, as shown in Fig. 9. It was observed that the degradation percentage is reduced as

compared to the initially used fresh Cu nanosheet powder. The reduction in degradation could be due to the decrease in Cu nanosheets' catalytic activity, possibly due to the aggregation of nanosheets in the synthetic dye solution.

The reaction kinetics of the degradation of methylene blue dye using Cu nanosheets under UV and solar light irradiation were explored and shown in Fig. 10. From the figure, it has been noticed that the dye degradation follows pseudo zero order kinetics for UV irradiation and the rate constant was found to be 0.66 whereas solar irradiation follows first order kinetics with a rate constant of 0.78 h^{-1}.

3.4. Photoluminescence study of Cu nanosheets

Fig. 11 represents the photoluminescence spectra of the synthesized Cu nanosheets obtained using a low intensity source in the UV-vis spectrum. Upon exciting the sample using
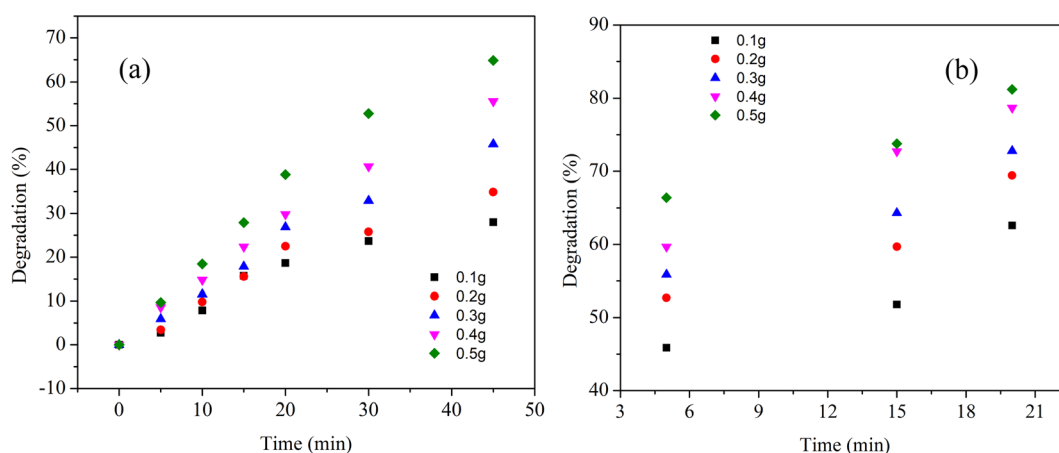

Fig. 9 Degradation of MB dye with recycled Cu nanosheet powder under (a) UV light and (b) solar light irradiation.
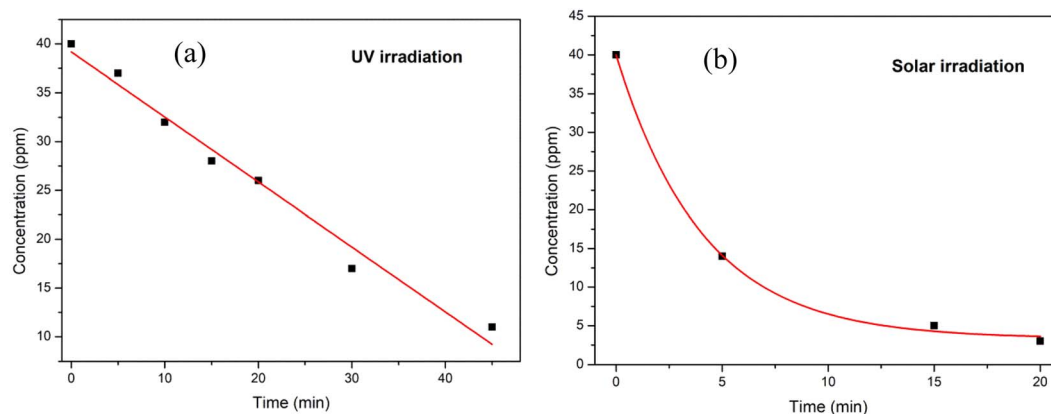
© 2022 The Author(s). Published by the Royal Society of Chemistry

Environ. Sci.: Adv., 2022, **1**, 814–826 | **821**

View Article Online

Environmental Science: Advances

Paper

Open Access Article. Published on 30 2022. Downloaded on 29/01/26 07:03:55. This article is licensed under a Creative Commons Attribution-NonCommercial 3.0 Unported Licence.

Fig. 10 Reaction kinetics model fitting for MB dye degradation under (a) UV light and (b) solar light irradiation.

a xenon laser, d-band electrons jumped into the sp-conduction band due to inter band transition. A peak at 535 nm from the photoluminescence plot confirms the recombination of electron hole pairs between the d-band and sp-conduction band which in turn produces luminescence. A similar type of result was also observed by other researchers.[42,43]

A summarized table describing various recent research findings on the Cu nanostructures and their application in dye degradation has been provided (Table 1). From the table, it can be observed that a very limited amount of work has been conducted on the application of pure Cu nanostructures to photocatalytic degradation of dyes. Also, the degradation time to achieve more than 95% efficiency is very high as compared to our work where it acquired ∼20 min using 2-D Cu nanostructures (Cu nanosheets reported in this work).

From the literature, it has been observed that most of the degradation of organic dye pollutants was performed by irradiating the waste water containing organic dye pollutants using UV and solar light in the presence of some semiconductor nanoparticles as photocatalysts such as ZnO and TiO$_2$. The nanostructures used in these studies are mostly zero dimensional nanostructures and exhibit less adsorption followed by less degradation upon irradiation. Also the time required for degradation is high for achieving maximum degradation efficiency. In contrast, in our current work reported here, the synthesized 2-dimensional Cu nanostructures act as an efficient photocatalyst upon irradiation as compared to zero dimensional nanostructures used in the literature. Due to their 2-dimensional structure, these photocatalysts create more active sites for adsorbing the pollutants thereby increasing the
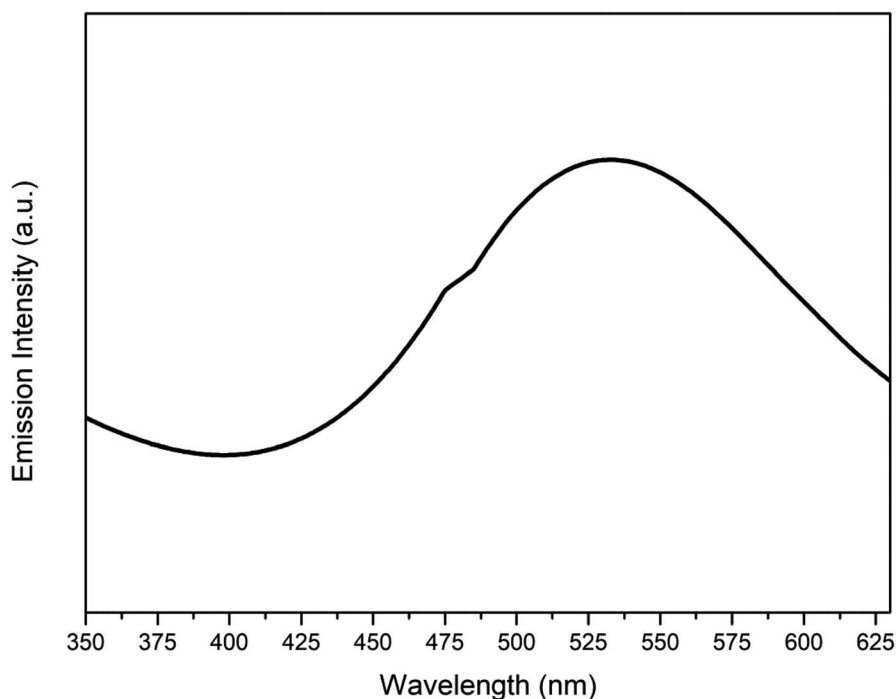

Fig. 11 Photoluminescence spectra of Cu nanosheets.

822 | *Environ. Sci.: Adv.*, 2022, **1**, 814–826

© 2022 The Author(s). Published by the Royal Society of Chemistry

Table 1 Table describing the comparison of various research findings from the literature on Cu nanostructures as an efficient photocatalyst in dye degradation with those from the current work

S. no	Type of Cu nanostructure	Name of the dye degraded	Type of irradiation	Degradation time	Degradation efficiency	Reference
1	Cu nanoparticles	Methylene blue (MB)	Solar	135 min	96%	Sinha and Ahmaruzzaman (2015)[44]
2	Cu doped ZnO nanoparticles	MB and methyl orange (MO)	Solar	30 min	92% for MB and 80% for MO	Kuriakose et al. (2015)[45]
3	Cu nanoparticles	MO and eosin	Without irradiation	45 hours	92% for MO and 95% for eosin	Kumar et al. (2021)[46]
4	Cu doped TiO$_2$	MB	Solar	120 min	99%	Ikram et al. (2020)[47]
5	Cu nanosheets	MB	Solar	20 min	95%	Our current work

degradation efficiency and reducing the time required for degradation as compared to conventional degradation methods. Moreover, they can also help in replacing other 2D nanostructured based photocatalysts such as graphene due to their economics in terms of synthesis of these structures. Graphene synthesis requires some autoclave reactors and high temperature which makes the product highly expensive. However, the Cu nanosheets prepared in this work do not require any autoclave reactors and high temperatures thereby making the product inexpensive.

3.5. Mechanism of MB dye degradation using Cu nanosheets

The probable charge carrier transfer mechanism for the degradation of methylene blue dye using Cu nanosheets is shown in Fig. 12. The energy band gap of the synthesized Cu nanosheets as observed from the Tauc plot is around 2.78 eV which lies in the visible range (1.7–3.1 eV) of electromagnetic spectra. When Cu nanosheets present in the MB dye solution are illuminated by the solar light, they absorb the photon energy which is equal to their energy band gap and generate the electrons and holes thereby promoting the transfer of electrons from the valence band to the conduction band leaving the holes in the valence band.[44,48] These electrons and holes present in the conduction band and valence band react with the available acceptor and donor species that are absorbed on the surface of the photocatalyst to produce superoxide and hydroxyl radicals. Since the Cu nanosheets have a large surface area due to their 2-dimensional structure, they provide more active sites for reacting the electrons and holes with acceptor and donor
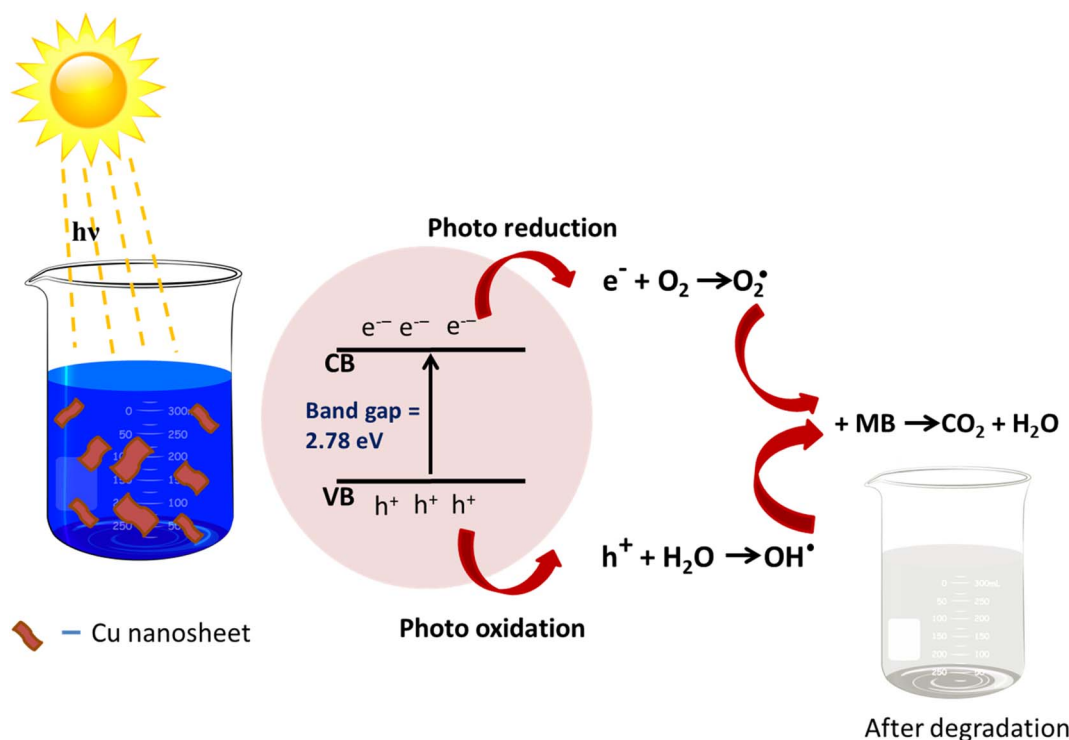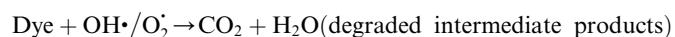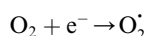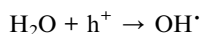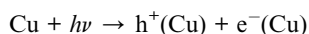

Fig. 12 Schematic representing the MB dye degradation mechanism using Cu nanosheets.

species and help in the generation of more superoxide and hydroxyl radicals. Then the formed radicals which are highly reactive in nature react with the dye and degrade the dye into non-toxic compounds. The following reactions suggest the mechanism of photodegradation of MB dye using Cu nanosheets.

$$Cu + h\nu \rightarrow h^+(Cu) + e^-(Cu)$$

$$H_2O + h^+ \rightarrow OH^\cdot$$

$$O_2 + e^- \rightarrow O_2^{\cdot-}$$

$$Dye + OH^\cdot/O_2^{\cdot-} \rightarrow CO_2 + H_2O (degraded\ intermediate\ products)$$

4. Conclusion

Two-dimensional Cu nanostructures such as nanosheets were successfully synthesized using a non-toxic reducing agent such as ascorbic acid and by replacing the conventional hydrothermal methods with simple and rapid chemical reduction techniques. The concentration of NaOH was successfully tuned to promote the growth of Cu nanosheets. The synthesized Cu nanosheets are highly resistant to oxidation even after exposure to air, as confirmed by the XRD analysis.

Cu nanosheets show excellent photocatalytic activity in degrading the methylene blue dye from the synthetic wastewater solution. The degradation efficiency increases as the concentration of Cu nanosheets in synthetic dye solution increases. Solar light irradiation exhibits higher degradation efficiency than UV light irradiation, possibly due to the higher intensity of solar light compared to that of UV light. The recycled Cu nanosheet powder from the centrifugation of the used dye solution shows better photocatalytic activity in degrading the fresh dye solution. Since these Cu nanosheets show an energy band gap of ~3 eV, they can be considered as an alternative for other semiconductor photocatalysts such as ZnO and TiO_2 in terms of organic pollutant removal. In addition, the Cu nanosheets photocatalyst can also be easily commercialised on par with graphene due to the low cost and simple, rapid technique in producing photocatalysts on a large scale.

Conflicts of interest

There are no conflicts to declare.

Acknowledgements

References

1 Y. Ye, B. Yu, Z. Gao, H. Meng, H. Zhang, L. Dai and G. Qin, Two-dimensional CdS nanosheet-based TFT and LED nanodevices, *Nanotechnology*, 2012, **23**, 194004.

2 H. L. Guo, X. F. Wang, Q. Y. Qian, F. B. Wang and X. H. Xia, A green approach to the synthesis of graphene nanosheets, *ACS Nano*, 2009, **3**, 2653–2659.

3 S.-Y. Son, J.-M. Yun, Y.-J. Noh, S. Lee, H.-N. Jo, S.-I. Na and H.-I. Joh, Highly flexible and bendable carbon nanosheets as transparent conducting electrodes for organic solar cells, *Carbon*, 2015, **81**, 546–551.

4 Y. G. Seol, T. Q. Trung, O. J. Yoon, I. Y. Sohn and N. E. Lee, Nanocomposites of reduced graphene oxide nanosheets and conducting polymer for stretchable transparent conducting electrodes, *J. Mater. Chem.*, 2012, **22**, 23759–23766.

5 P. Long, Z. Zhang, G. Peng, Q. Zhang, D. Liu, X. Xu and X. Yao, Facile synthesis of Co9S8 nanosheets for lithium ion batteries with enhanced rate capability and cycling stability, *New J. Chem.*, 2017, **41**, 9184–9191.

6 S. Wang, L. Wang, K. Zhang, Z. Zhu, Z. Tao and J. Chen, Organic $Li_4C_8H_2O_6$ Nanosheets for Lithium-Ion Batteries, *Nano Lett.*, 2013, **13**, 4404–4409.

7 K. Zhao, S. Liu, G. Ye, Q. Gan, Z. Zhou and Z. He, High-yield bottom-up synthesis of 2D metal-organic frameworks and their derived ultrathin carbon nanosheets for energy storage, *J. Mater. Chem. A*, 2018, **6**, 2166–2175.

8 J. Xu, J. Zhang, W. Zhang and C. S. Lee, Interlayer nanoarchitectonics of two-dimensional transition-metal dichalcogenides nanosheets for energy storage and conversion applications, *Adv. Energy Mater.*, 2017, **7**, 1–30.

9 X. Yu, P. Han and Y. Li, Oxidative desulfurization of dibenzothiophene catalyzed by α-MnO_2 nanosheets on palygorskite using hydrogen peroxide as oxidant, *RSC Adv.*, 2018, **8**, 17938–17943.

10 A. H. Shaik, S. Shaik, S. Goyal, M. R. Chandan, I. Veza, A. Buradi and I. M. Alarifi, A Review on Environmental and Economic Impact of 2D Nanomaterials-Based Heat Transfer Fluids, *J. Nanomater.*, 2022, **2022**, 3443360.

11 P. Martínez-Merino, E. Sani, L. Mercatelli, R. Alcántara and J. Navas, WSe_2 Nanosheets Synthesized by a Solvothermal Process as Advanced Nanofluids for Thermal Solar Energy, *ACS Sustain. Chem. Eng.*, 2020, **8**, 1627–1636.

12 B. Cao, W. Cai, Y. Li, F. Sun and L. Zhang, Ultraviolet-light-emitting ZnO nanosheets prepared by a chemical bath deposition method, *Nanotechnology*, 2005, **16**, 1734–1738.

13 J. Zhao, C. Ye, X. Fang, P. Yan, Z. Wang and L. Zhang, Synthesis of single crystalline cadmium nanosheets by a thermal decomposition method, *J. Cryst. Growth*, 2005, **277**, 445–449.

14 Q. Xiao, S. Huang, J. Zhang, C. Xiao and X. Tan, Sonochemical synthesis of ZnO nanosheet, *J. Alloys Compd.*, 2008, **459**, 18–22.

15 D. Sahoo, B. Kumar, J. Sinha, S. Ghosh, S. S. Roy and B. Kaviraj, Cost effective liquid phase exfoliation of MoS_2

nanosheets and photocatalytic activity for wastewater treatment enforced by visible light, *Sci. Rep.*, 2020, **10**, 1–12.

16 L. Tang, X. Li, R. Ji, K. S. Teng, G. Tai, J. Ye, C. Wei and S. P. Lau, Bottom-up synthesis of large-scale graphene oxide nanosheets, *J. Mater. Chem.*, 2012, **22**, 5676–5683.

17 D. P. Dubal, D. S. Dhawale, R. R. Salunkhe, V. S. Jamdade and C. D. Lokhande, Fabrication of copper oxide multilayer nanosheets for supercapacitor application, *J. Alloys Compd.*, 2010, **492**, 26–30.

18 S. Wang, Z. Chen, I. Cole and Q. Li, Structural evolution of graphene quantum dots during thermal decomposition of citric acid and the corresponding photoluminescence, *Carbon*, 2015, **82**, 304–313.

19 K. Krishnamoorthy, G. S. Kim and S. J. Kim, Graphene nanosheets: ultrasound assisted synthesis and characterization, *Ultrason. Sonochem.*, 2013, **20**, 644–649.

20 Y. Li, X. Yin and W. Wu, Preparation of Few-Layer MoS_2 Nanosheets via an Efficient Shearing Exfoliation Method, *Ind. Eng. Chem. Res.*, 2018, **57**, 2838–2846.

21 A. H. Shaik and J. Chakraborty, A simple room temperature fast reduction technique for preparation of a copper nanosheet powder, *RSC Adv.*, 2016, **6**, 14952–14957.

22 S. Lee, S. Wang, C. Wern and S. Yi, The Green Synthesis of 2D Copper Nanosheets and Their Light Absorption, *Materials*, 2021, **14**, 1926.

23 S. R. Manippady, A. Singh, B. M. Basavaraja, A. K. Samal, S. Srivastava and M. Saxena, Iron-Carbon Hybrid Magnetic Nanosheets for Adsorption-Removal of Organic Dyes and 4-Nitrophenol from Aqueous Solution, *ACS Appl. Nano Mater.*, 2020, **3**, 1571–1582.

24 W. Lei, D. Portehault, D. Liu, S. Qin and Y. Chen, Porous boron nitride nanosheets for effective water cleaning, *Nat. Commun.*, 2013, **4**, 1–7.

25 Z. Wang, K. Wang, Y. Wang, S. Wang, Z. Chen, J. Chen and J. Fu, Large-scale fabrication of N-doped porous carbon nanosheets for dye adsorption and supercapacitor applications, *Nanoscale*, 2019, **11**, 8785–8797.

26 H. Dang, L. Chen, L. Chen, M. Yuan, Z. Yan, M. Li, L. Chen, L. Chen, M. Yuan, Z. Yan and M. Li, Hydrothermal synthesis of 1T-WS2 nanosheets with excellent adsorption performance for dye removal from wastewater, *Mater. Lett.*, 2019, **254**, 42–45.

27 N. M. Mahmoodi and M. H. S. Dastgerdi, Clean Laccase immobilized nanobiocatalysts (graphene oxide - zeolite nanocomposites): from production to detailed biocatalytic degradation of organic pollutant, *Appl. Catal., B*, 2020, **268**, 118443.

28 N. M. Mahmoodi, F. Najafi and A. Neshat, Poly(amidoamine-co-acrylic acid) copolymer: synthesis, characterization and dye removal ability, *Ind. Crops Prod.*, 2013, **42**, 119–125.

29 N. M. Mahmoodi, B. Hayati, H. Bahrami and M. Arami, Dye adsorption and desorption properties of Mentha pulegium in single and binary systems, *J. Appl. Polym. Sci.*, 2011, **122**, 1489–1499.

30 N. M. Mahmoodi, Synthesis of magnetic carbon nanotube and photocatalytic dye degradation ability, *Environ. Monit. Assess.*, 2014, **186**, 5595–5604.

31 N. M. Mahmoodi, A. Taghizadeh, M. Taghizadeh and M. S. Baglou, Surface modified montmorillonite with cationic surfactants: preparation, characterization, and dye adsorption from aqueous solution, *J. Environ. Chem. Eng.*, 2019, **7**, 103243.

32 B. Hayati, N. M. Mahmoodi and A. Maleki, Dendrimer–titania nanocomposite: synthesis and dye-removal capacity, *Res. Chem. Intermed.*, 2015, **41**, 3743–3757.

33 B. Hayati, N. M. Mahmoodi, M. Arami and F. Mazaheri, Dye Removal from Colored Textile Wastewater by Poly(propylene imine) Dendrimer: Operational Parameters and Isotherm Studies, *Clean: Soil, Air, Water*, 2011, **39**, 673–679.

34 M. Oveisia, M. A. Asli and N. M. Mahmoodi, Carbon nanotube based metal-organic framework nanocomposites: synthesis and their photocatalytic activity for decolorization of colored wastewater, *Inorg. Chim. Acta*, 2019, **487**, 169–176.

35 A. Almasian, M. E. Olya and N. M. Mahmoodi, Preparation and adsorption behavior of diethylenetriamine/polyacrylonitrile composite nanofibers for a direct dye removal, *Fibers Polym.*, 2015, **16**, 1925–1934.

36 N. M. Mahmoodi, M. Oveisia, M. Bakhtiaria, B. Hayati, A. A. Shekarchi, A. Bagheri and S. Rahimi, Environmentally friendly ultrasound-assisted synthesis of magnetic zeolitic imidazolate framework - graphene oxide nanocomposites and pollutant removal from water, *J. Mol. Liq.*, 2019, **282**, 115–130.

37 N. M. Mahmoodi, M. Bashiri and S. J. Moeen, Synthesis of nickel–zinc ferrite magnetic nanoparticle and dye degradation using photocatalytic ozonation, *Mater. Res. Bull.*, 2012, **47**, 4403–4408.

38 M. R. Chandan, S. Goyal, M. Rizwan, M. Imran and A. H. Shaik, Removal of textile dye from synthetic waste-water using microporous polymer nanocomposite, *Bull. Mater. Sci.*, 2021, **44**, 272.

39 M. R. Chandan, K. Radhakrishnan, D. K. Bal and A. H. Shaik, Flexible polyurethane foam-ZnO nanocomposite for photocatalytic degradation of textile dye, *Fibers Polym.*, 2020, **21**, 2314–2320.

40 A. H. Shaik and J. Chakraborty, Use of repeated phase transfer for preparation of thiol coated copper organosols at higher particle loading, *Colloids Surf., A*, 2014, **454**, 46–56.

41 Y. Wang, J. Zhang, Y. Yang, F. Huang, J. Zheng, D. Chen, F. Yan, Z. Lin and C. Wang, NaOH Concentration Effect on the Oriented Attachment Growth Kinetics of ZnS, *J. Phys. Chem. B*, 2007, **111**, 5290–5294.

42 Y. B. Soskovets, A. Y. Khairullina and V. A. Babenko, Photoluminescence spectra of copper-based planar nanostructures, *J. Appl. Spectrosc.*, 2006, **73**, 576–582.

43 R. Das, S. S. Nath and R. Bhattacharjee, Luminescence of copper nanoparticles, *J. Lumin.*, 2011, **131**, 2703–2706.

44 T. Sinha and M. Ahmaruzzaman, Green synthesis of copper nanoparticles for the efficient removal (degradation) of dye from aqueous phase, *Environ. Sci. Pollut. Res. Int.*, 2015, **22**, 20092–20100.

© 2022 The Author(s). Published by the Royal Society of Chemistry

Environ. Sci.: Adv., 2022, **1**, 814–826 | **825**

45 S. Kuriakose, B. Satpatib and S. Mohapatra, Highly efficient photocatalytic degradation of organic dyes by Cu doped ZnO nanostructures, *Phys. Chem. Chem. Phys.*, 2015, **17**, 25172.

46 S. R. Kumar, M. Vanaja and A. Kalirajan, Degradation of Toxic Dye Using Phytomediated Copper Nanoparticles and Its Free-Radical Scavenging Potential and Antimicrobial Activity against Environmental Pathogens, *Bioinorg. Chem. Appl.*, 2021, **2021**, 1222908.

47 M. Ikram, E. Umar, A. Raza, A. Haider, S. Naz, A. Ul-Hamid, J. Haider, I. Shahzadi, J. Hassan and S. Ali, Dye degradation performance, bactericidal behavior and molecular docking analysis of Cu-doped TiO2 nanoparticles, *RSC Adv.*, 2020, **10**, 24215–24233.

48 M. Usman, A. Ahmed, B. Yu, Q. Peng, Y. Shen and H. Cong, Photocatalytic potential of bio-engineered copper nanoparticles synthesized from Ficus carica extract for the degradation of toxic organic dye from waste water: growth mechanism and study of parameter affecting the degradation performance, *Mater. Res. Bull.*, 2019, **120**, 110583.